



37 and prediction of future, climate development. Loess–paleosol sequences are now
38 recognized as one of the most complete terrestrial records of glacial–interglacial
39 cycles of the Quaternary Period (Porter, 2001; Muhs and Bettis, 2003, Pierce et al,
40 2011).

41 Aeolian sediments with paleosol layer enumerate as a best sediment records for
42 paleoclima especially for Quaternary evidence in continents (Guo et al, 2002).
43 Loess/paleosols sequence are one of the important natural climate change archives
44 in continents and have been used for reconstruction of Quaternary climate and
45 geomorphological changes (Karimi et al., 2011; Frechen et al., 2003; Prins et al.,
46 2007).

47 Loess deposits have covered large areas of the northeast, east central, north and
48 central parts of Iran which are part of loess belt that cover the Middle East and
49 extend further northward into Turkmenistan, Qazakistan and Tajikistan (Okhravi
50 and Amini, 2001).The extensive and thick loess deposits in northern Iran have been
51 recently studied in detail setting up a more reliable chronological framework for the
52 last interglacial/glacial cycle (Lateef, 1988; Pashae, 1996; Kehl et al., 2006;
53 Frechen et al., 2009, Karimi et al, 2009, Karimi et al, 2013, Okhravi and Amini,
54 2001, Mehdipour et al, 2012).

55 Paleoclimatical studies of loess deposits based on rock magnetism and
56 combination of magnetism and geochemistry of loesses around the world have
57 attained appreciable advances in the past few decades (Heller and Liu, 1984; Forster
58 et al., 1996; Ding et al., 2002; Guo et al., 2002; Chlachula, 2011; Bronger, 2003;
59 Baumgart et al., 2013, Guanhua, et al, 2014).

60 These provide a relatively loess-paleosols sequence records that cover the area of
61 Chinas loess plateaus, Germany, Poland, Tajikestan, Austrian, Ukraine, Danube
62 catchment (Hosek et al, 2015,Ahmad and Chandra, 2013, Chen, 2010; Jordanova et
63 al., 2011; Buggle et al., 2009; Fitzsimmons et al., 2012; Fischer et al., 2012; Jary
64 and Ciszek, 2013; Baumgart et al., 2013; Schatz et al., 2014; Gocke et al., 2014).

65 Geographical latitude of North of Iran is similar to middle Asia and China.

66 These are very limited records of concerning loess deposits of Iran in compare to
67 other places of world, and therefore this study attempt to explore the potential of
68 loess deposits in reconstruction of northern Iran during late quaternary.

69

70 **Study area**

71 The Nowdeh section is exposed at about 20 km southeast of Gonbad-e Kavus and
72 east of Azadshahr city. The Nowdeh river dissects more than 24 m thick sequence

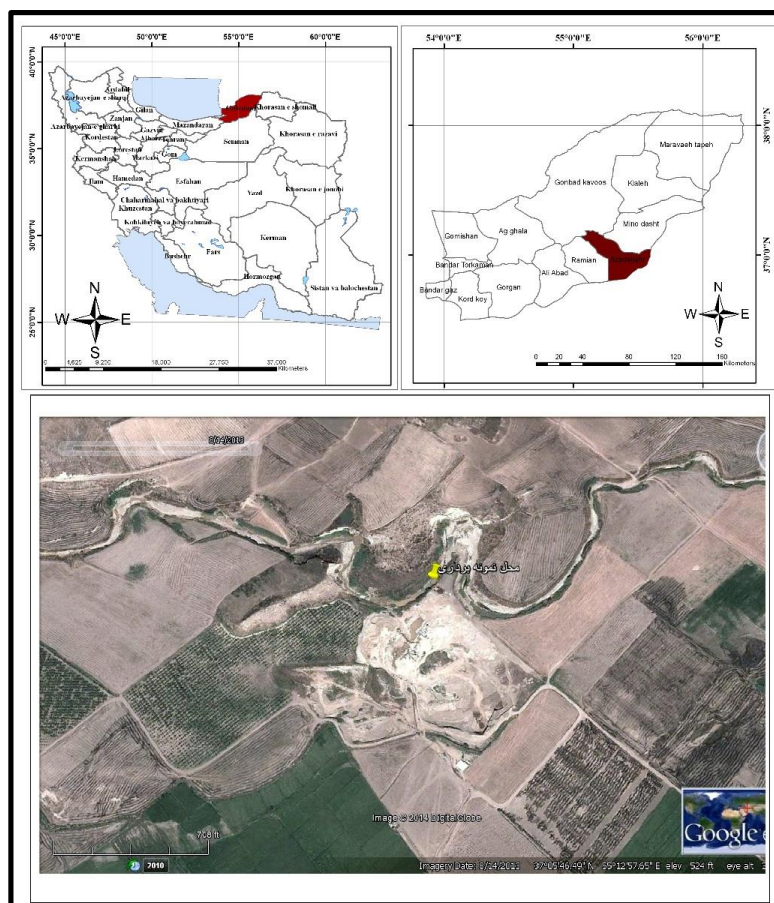


73 of dull yellowish brown (10 YR 5/4) loess covering northeast weathered limestone
74 dipping.

75 The study area falls between 37° 05' 50" N and 55° 12' 58"E coordinates. This
76 section is in Alborz structure and its sediment sheet includes of north of Caspian
77 Sea. Nabavi (1976) said that "sediment structure of this section is in Gorgan-Rasht
78 zone and Paratetis district". This zone includes of regions that locate in north of
79 Alborz fault and south of Caspian Sea. Toward the east, Gorgan-Rasht zone cover
80 with thick layers of loess.

81 Attention to above statements, deal with to identifying of segment for sampling.
82 After searching, Nowdeh section that has been used for soil study in before years by
83 Kehl et al (2005) and Frichen et al (2009) were selected. One of another reason to
84 selection this section was having 12 dating that have done in before studies
85 (Figure1).

86



87
88

Figure 1: Map of Iran and the location of Nowdeh loess-paleosol sequence.



89

90 **Methodology**

91 In this study, Azadshar (Nowdeh Loess Section) was selected to reconstruct Late Quaternary
92 climate change in the north Iran. The Nowdeh loess section with an about 24 m thickness were
93 sampled in detailed 10 cm intervals with magnetometry and geochemical of the analysis. For this
94 aim, sampling location and method was determined after consecutive study area. Magnetic
95 susceptibility of all samples was measured in Environmental and Paleomagnetic laboratory based
96 at Geological Survey of Iran, Tehran, Iran. The magnetic susceptibility represents the integrated
97 response of diamagnetic, paramagnetic, ferrimagnetic and imperfect antiferromagnetic minerals.
98 All samples were placed in an 11 cm³ plastic cylinders to be used in magnetic measurement
99 instruments. Magnetic susceptibility was measured using AGICO company made Kappabridge
100 model MFK1-A instrument.

101 Saturation isothermal remnant magnetization (SIRM) were determined which reflects the
102 concentration of ferromagnetic and imperfect antiferromagnetic minerals. The HIRM ('hard'
103 isothermal remanence) magnetization is calculated to determine the magnetically based
104 component such as hematite in samples following the formula:

$$105 \text{ HIRM} = 0.5(\text{SIRM} + \text{IRM}_{-0.3\text{T}})$$

106 Where $\text{IRM}_{-0.3\text{T}}$ is the remanence after application of a reversed field of 0.3 T after growth and
107 measurement of SIRM. The HIRM reflects the contribution specifically of the imperfect
108 antiferromagnetic minerals hematite and goethite (Bloemendal *et al.*, 2008).

109 The $S_{-0.3\text{T}}$ value, or $S_{\text{-ratio}}$, is calculated as

$$110 S_{-0.3\text{T}} = 0.5[(-\text{IRM}_{-0.3\text{T}}/\text{SIRM}) + 1]$$

111 And is ranged between 0 and 100%. It reflects the ratio of ferrimagnetic to imperfect
112 antiferromagnetic minerals (Bloemendal *et al.*, 2008).

113 Base on the results of magnetic susceptibility, the geochemical proxies of chemical weathering of
114 selected 70 samples (trace elements) are included to assist the paleoclimatic interpretation of the
115 magnetic signals.

116

117 **Results**

118 **Magnetic properties**

119 Figure 2 show relationship of susceptibility, NRM, SIRM, HIRM and $S_{-0.3\text{T}}$ in
120 Nowdeh section. The variation of magnetic susceptibility signal in the Nowdeh
121 section suggests variation in climate conditions and mechanisms during the Late
122 Quaternary. The rock magnetic records correlate well with the lithology in Nowdeh



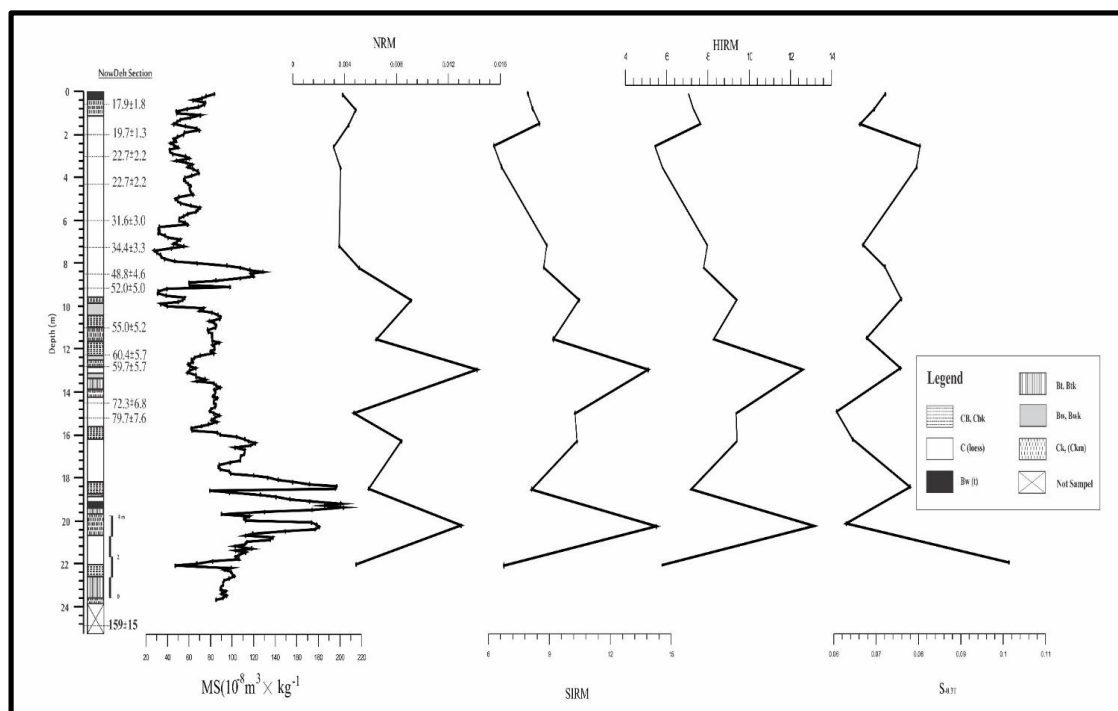
123 section. In general, the paleosols are characterized by an enhancement of the
124 magnetic signal compared to loess. The values of χ (in $10^{-8} \text{ m}^3 \text{ kg}^{-1}$) vary from
125 28.17 to 203.13 in Nowdeh section. Maximum χ values (203.13) occur in the lower
126 paleosol layer (19.4 m) and minimum values occur in the top loess layer (7.4 m).

127 The variance of this parameter is at the depth of 22-23.7 m and had a salient decrease
128 at the depth 22.1 m. Then the variation range decrease until 20 meter of depth. Severe
129 variation of magnetic susceptibility has been observed at the depth of 20 to 16 m.
130 After that χ decrease until 16 to 10 m of depth and then again variation in χ has
131 observed from 10 to 8 meter of depth respectively.

132 Paleosols showing higher values of χ than loesses, where the magnetic enhancement
133 occurs in the Bw, Bt, Btk, whereas the underlying C (loess) horizon is characterized
134 by lower values of χ . This is very likely caused by the precipitation of iron oxides in
135 Bw horizon and consequently a higher amount of pedogenetic magnetite in
136 comparison with the C horizon can be observed (Jordanova et al., 2013, Hosek et al,
137 2015). The χ -values of the lower and middle part of Nowdeh section, approximately
138 53-80 and 120-140 Ka representing intermediate values between unweathered
139 loesses and weathered paleosols.

140 The results showed that NRM is consonant with magnetic susceptibility variance.
141 This consonant variation especially is so in lower depth and the highest record of
142 this parameter occurred in 13.1 meter of earth surface that posed in BW, BWK
143 horizon. Variations and differences in magnetic susceptibility are very agreed with
144 SIRM of Loess sequence. As magnetic susceptibility decrease, SIRM also decrease
145 and overhand. Between the 20 to 50 ka, which most of upper Loess has formed, the
146 magnetic susceptibility show no variation likewise SIRM diagram show that in this
147 median. High value of HIRM in fig 2 reflects concentration and frequencies of
148 magnetic deterring minerals such as Goethite, maghemite or hematite has increased.

149 Comparison of lower values of $S_{(-0.3T)}$ (between 0.6 to 0.12 Am/m) and higher value
150 of HIRM (between 2 to 5 Am/m) show that the ratio of minerals with lower (such as
151 magnetite) is very lower than the ratio of minerals with high in paleosols. This is in
152 contrast with loess deposit.



153

154

Figure 2: Basic magnetic parameters for Nowdeh section.

155 Element stratigraphy

156 Figure 3 shows correlation between concentration of selected element (Sr, Rb, Zr,
157 Ti and Mn) and magnetite susceptibility in Nowdeh section.

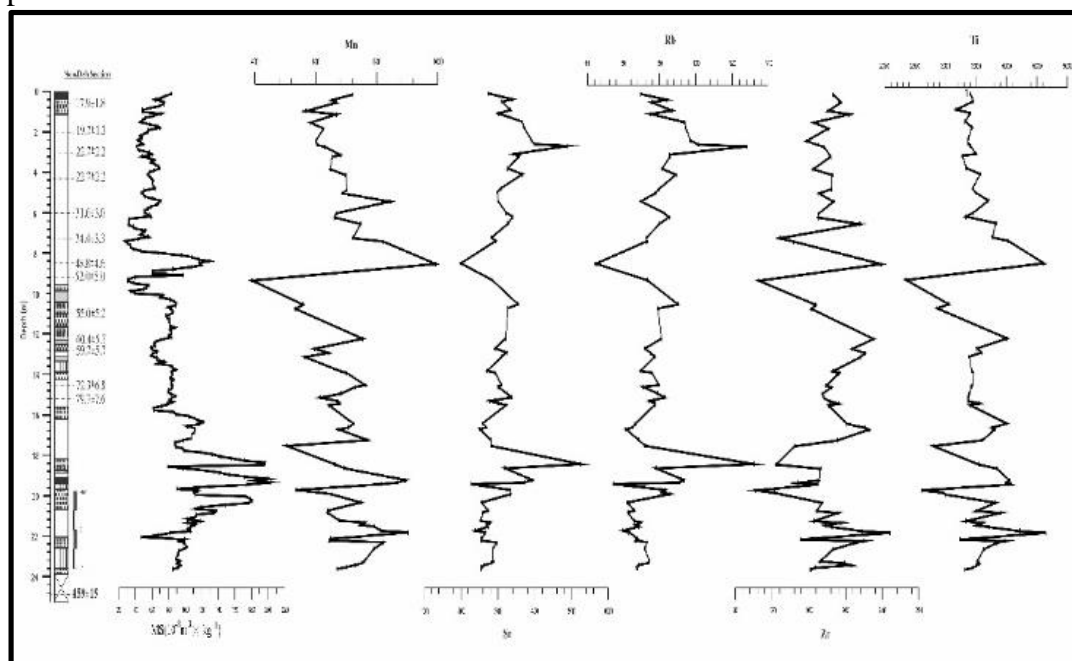
158 As it is clear from this figure variation in concentration of these elements are
159 high with differences in between. Sr and Rb have similar trend along Nowdeh
160 section. At the depth of 2.9 m of depth, there is an increase in concentration of these
161 two elements. Which corresponds with an age of 22 ka. The concentration of these
162 two elements is decreased right after this point.

163 The lower concentration of elements has recorded at the depth of 8.5 meter with 48.8
164 ka in age. There is no variation in concentration of these elements after this depth
165 (8.5 meter) in concentration of these elements have occurred at the depth of 18
166 meters. These elements is the highest record of concentration in Nowdeh section.

167 Ti, Zr and Mn show approximately similar trend in diagram. These elements show
168 little variation in concentration in outset of the section.



169 But from depth of 6.2 meter and with an age of to31.1. The variation in concentration
170 begin to increase and attain the highest value in this zone. Concentration of these
171 element at the depth of 8.5 m (34.4 ka). Followed by decrease at the depth of 9.3
172 meter, are the main elements in this part of Nowdeh section. This is a little variation
173 in concentration of these elements up to the depth of 16.7 meter. From the depth of
174 16.7 m up to the bottom of the section in concentration of elements show zig-zag
175 pattern.



176
177 Figure 3: shows depth series of selected element concentrations for Nowdeh section.

178 Trace element ratio

179 The variation of Si/Ti ratio is following magnetic susceptibility except for lower part
180 of the section (23-24m). The variation of Mn/Sr, Zr/Ti and Mn/Ti almost show no
181 change except for depth 8.5 m corresponding to 48.8 ka in age. The variation of
182 Rb/Sr ratio is almost opposite of MS pattern especially at the depth of 8.5, 16, 19
183 and 22 m. the variation of Ba/Rb ratio is also following MS pattern except at depth
184 of 13,15, 19 and 22.8 m which are opposite to each other. Figure 4 show depth series
185 of selected element ratio concentrations for the Nowdeh section with the frequency
186 dependent magnetic susceptibility.



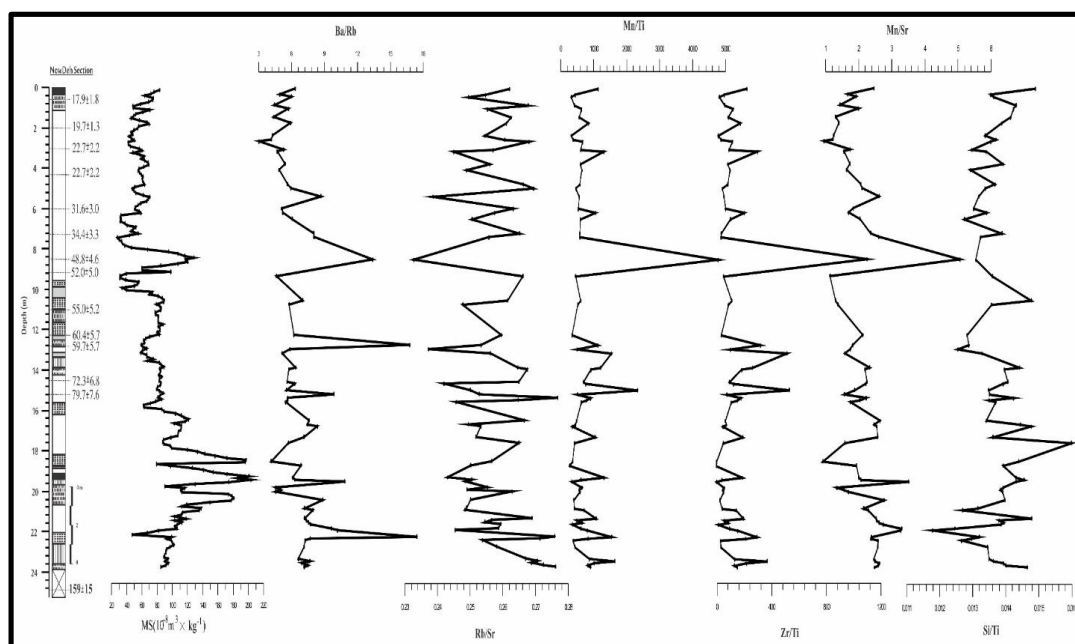
187 Si/Ti variation in these ratio do not show any consistent relationship to the sequence
188 of loess/palaeosol layers (as defined by the magnetic susceptibility) at Nowdeh
189 section. Mn/Ti — this ratio tend to be show elevated values in the palaeosols,
190 probably as the result of the concentration of Mn oxide in the finer sediment
191 fraction(Bloemendal , et al, 2008).

192
193 Zr/Ti, Mn/Ti, Rb/Sr and Mn/Sr—the curves of these ratios show a very clear pattern
194 of elevation in the palaeosols, and their high degree of similarity is noteworthy.
195 Rb/Sr has been proposed by several workers as an indicator of pedogenic intensity
196 for loess based on the differential weather ability of the major host minerals — K-
197 feldspar for Rb and carbonates for Sr. In the case of Mn/Sr, the higher value in the
198 palaeosol will result from the effect of grain-size on the Mn concentration, as noted
199 above, and the solution loss of Sr.

200 Chen et al. (1999) compared Rb/ Sr and magnetic susceptibility in the uppermost
201 (last glacial/interglacial) parts of the Luochuan and Huanxian sections, and found a
202 striking correspondence between the amplitudes of variation in magnetic
203 susceptibility and in Rb/Sr.

204 In deep of 19/4m, which is often referenced as a strongly developed palaeosol and
205 which is taken to represent an interval of warm and humid climate and magnitude
206 susceptibility is higher, shows only moderate Rb/Sr ratios.

207



208

209

Figure 4: show selected element ratios in Nowdeh section



210 Discussion

211 Considering the entire 159 Ka sequence at the Nowdeh site there is reasonable first
212 order co-variation of the magnetic and geochemical indicators of weathering and soil
213 formation – especially in the case of magnetic parameters reflecting variations in
214 ferrimagnetic content and the Sr based ratios. However, detailed comparison on the
215 basis of individual loess and palaeosol layers shows that there is an inconsistent
216 relationship between the amplitudes of individual peaks and troughs of magnetic and
217 geochemical parameters.

218 Therefore, suggestions by some workers of a consistent loess magnetic
219 mineralogical and geochemical response to weathering and soil formation clearly
220 possible on the post 159 Ka period.

221
222

223 For identification of relationship between climate change and magnetic properties
224 of sediments, magnetic susceptibility of loess sediments in Nowdeh section
225 experimented. Nowdeh magnetic susceptibility results showed cold and dry and
226 warm and humid sequence that related to Loess-paleosol sequence respectively.

227 Sediment loess formed in cold and dry climate conditions that have low magnetic
228 susceptibility. Whereas in paleosols regarding to pedogenesis process, amount of
229 oxidation increase and so magnetic susceptibility records increase. Accordance to
230 global standard, always in loess/paleosol sequence, paleosols has higher magnetic
231 susceptibility than adjacent loess. (Song et al, 2008).

232 Because pedogenesis possess accrete to strong magnetic minerals formation of Iron
233 Oxide in soils includes of; Fe_3O_4 , $\gamma\text{-Fe}_2\text{O}_3$, $\text{Fe}_2\text{O}_3 - \alpha$. Whereas mineral magnetic
234 of Loess layer related to grain variation of aeolian resource.

235 Regarding to fig 3, brown layers sequence of dark and light paleosols in Loess
236 demonstrate different process of weather that it is so similar to glacial and
237 interglacial periods in middle and last of Pleistocene. Paleosol of Nowdeh section
238 has higher magnetic susceptibility than loess. This content has seen more in low and
239 old depth that mean of high weather variation on that season. In 21 meter in depth
240 magnetic susceptibility has a considerable decreasing that indicate a cold and dry
241 season in this time. Also regarding to magnetic susceptibility chart, in Nowdeh
242 section magnetic susceptibility increasing has been seen in about of 8 periods. This
243 indicate temperature and humidity increasing in these times. In each section of



244 standard global Loess, always, regarding to pedogenes and oxidation, paleosoles
245 have higher in magnetic susceptibility than adjacent Loess layers (Maher, 2011).

246 Loess units formed in cold and dry weathering periods and mineral magnetic
247 resource belong to Aeolian sediments. Whereas, because of magnetic susceptibility
248 content increasing in paleosols, plus mineral magnetic with Aeolian resource,
249 mineral magnetic (iron oxide of soil) of sediments weathering should form by
250 improvement of paleosole formation. Studies and researches achievement on
251 magnetic susceptibility confirm this purports (Maher, 2011,. Spassov, 2002).

252 Fig 4 show that magnetic field intensity in cold glacial periods (time of loess layering)
253 is different with magnetic field intensity in warm interglacial periods (time of
254 paleosole formation). Results of NRM indicate it's decreasing by loess formation
255 and it's increasing by paleosols formation. This illustrate relationship between
256 natural remnant and magnetic susceptibility. So, NRM decreasing express dry and
257 cold weather condition that is concomitant with loess layers sedimentation. NRM
258 increasing either represent warm and humid weather conditions.

259 There are two probable reasons for Justification of magnetic susceptibility and
260 isothermal remnant magnetization low alternation in 20 t0 50 years ka that includes
261 of

- 262 1. Pedogenes process reduce because of cold and dry period
- 263 2. Reducing magnetic entering to loess layers

264 One of another magnetic susceptibility and isothermal remnant magnetization
265 coincidence is related to 20 last year's ka. Regarding to magnetic susceptibility
266 variation in surface layer of soil can say that probably this period of time accordance
267 to compietion of cold weather and todays weather creation in north of Iran (warm
268 and humid) and SIRM content has increased. Because of SIRM samples just selected
269 at peak point of magnetic susceptibility so, they don't show details of variations.

270 The comparison of results of this research with the results of Antoine et al., (2013)
271 on Loess/paleosol sediments of Central Europe, show a close relationship especially
272 at an age of 32 Ka, which show a climate change has taken place at this age. In both
273 sections, this change is recorded by decreasing in magnetic susceptibility



274 approximately in 30 Ka, at the base of deposition of loess, indicating dry and cold
275 climate in this period and increase in in magnetic susceptibility in 32 Ka, which
276 means appearance of warm and moist climate.

277 Geochemical chart can use as weather indexes. Because they can display various
278 weathering with different severity. In loess studies, there are several chemical ratio
279 that can use for reconstruction of paleoclima variations (Ding et al., 2001)=

280 Mn, Zr and Ti—variations in the bulk concentrations of soil elements show a straight
281 forward pattern of stratigraphic variability with higher values in the palaeosols and
282 lower values in the loess layers (Bloemendal et al., 2008). This reflects in part
283 carbonate dilution/concentration effects, since a significant amount of the variability
284 disappears when the elements are expressed on a carbonate-corrected basis.

285

286 In Nowdeh section, amount of Rb in paleosols was lower than its amount on loess
287 layers. This occur by high soluble capability of Rb in warm and humid climate
288 conditions as interglacial period. Gallet et al. (1996) found that Rb was significantly
289 depleted in the palaeosols.

290 Our results show that Mn/Ti, Zr/Ti and Mn/Sr ratios tend to be show higher values
291 in the palaeosols. Ding et al., 2001said that Mn/Ti has had elevated values in the
292 palaeosols, probably as the result of the concentration of Fe and Mn oxides in the
293 finer sediment fractions. Also, they said that Rb/Sr and Mn/Sr ratios curves show a
294 very clear pattern of elevation in the palaeosols same as results of this study. Rb/Sr
295 has been proposed by several workers as an indicator of pedogenic intensity for loess
296 based on the differential weatherability of the major host minerals — K-feldspar for
297 Rb and carbonates for Sr. Mn/Sr, the higher values in the palaeosols will result from
298 the effect of grain-size on the Mn concentrations, as noted above, and the solutinal
299 loss of Sr.

300 Chen et al. (1999) compared Rb/Sr and magnetic susceptibility in the uppermost (last
301 glacial/interglacial) parts of the Luochuan and Huanxian sections, and found a
302 striking correspondence between the amplitudes of variation in magnetic
303 susceptibility and in Rb/Sr (Bloemendal et al., 2008).

304

305 **Conclusion**



306 Loess/paleosols sequences from Northeastern of Iran provide a suitable archive for
307 a detailed study of the Upper Pleistocene paleoenvironmental changes. Using a
308 multi-proxy approach combining sedimentological, magnetic and geochemical
309 methods—we demonstrate that:

- 310 • The stratigraphy of the studied section conform well to the general pattern of
311 the Upper Pleistocene loess/paleosol successions in the relatively loess of
312 Northeastern of Iran.
- 313 • Because of high relationship between magnetic minerals and climate
314 conditions, magnetic parameters are an efficient variables for reconstruction
315 of climate change.
- 316 • Comparison of magnetic and geochemical charts show that the results of
317 geochemical weathering ratio variations are same as magnetic weathering
318 parameters variations such as magnetic susceptibility.
- 319 • High degree of coherency between the amplitudes of magnetic susceptibility
320 and Rb/Sr, Mn/Ti, Zr/ Ti and Mn/ Sr ratio are confirmed.

321

322 References

- 323 1. Ahmad, I., Chandra, R., 2013, Geochemistry of loess-paleosol sediments of Kashmir
324 Valley, India: Provenance and weathering, *Journal of Asian Earth Sciences* 66, 73-89.
- 325 2. Antoine, P., Rousseau, D.D., Degeai, J.P., Moine, O., Lacroix, O., Kreutzer, S., Fuchs, M., Hatte,
326 CH., Gauthier, C., Svoboda, J, and Lisa , I., 2013, High-resolution record of the environmental
327 response to climatic variations during the Last Interglacial Glacial cycle in Central Europe: the
328 loess-palaeosol sequence of Dolní Věstonice (Czech Republic), *Quaternary Science Reviews*, 67,
329 PP 17-38.
- 330 3. Baumgart, P., Hambach, U., Meszner, S., Faust, D., 2013. An environmental magnetic
331 fingerprint of periglacial loess: records of Late Pleistocene loess paleosol sequences from
332 Eastern Germany. *Quat. Int.* 296, 82–93.
- 333 4. Bloemendal, J., Xiuming L., Youbin, S., Ningning L., 2008. An assessment of magnetic
334 and geochemical indicators of weathering and pedogenesis at two contrasting sites on the
335 Chinese Loess plateau, *Palaeogeography, Palaeoclimatology, Palaeoecology* 257 ; 152–
336 168.
- 337 5. Bronger, A., 2003. Correlation of loess-paleosol sequence in East and Central Asia with
338 SE Central Europe: toward a continental Quaternary pedostratigraphy and paleoclimate
339 history. *Quaternary International* 106/107, 11–31.
- 340 6. Buggle, B., Hambach, U., Glaser, B., Gerasimenko, N., Markovic, S., Glaser, I., Zöller, L.,
341 2009. Stratigraphy, and spatial and temporal paleoclimatic trends in Southeastern/Eastern
342 European loess–paleosol sequences. *Quat. Int.* 196, 186–206.
- 343 7. Chen, J., An, Z.S., Head, J., 1999. Variation of Rb/Sr ratios in the loess–paleosol sequences
344 of central China during the last 130,000 years and their implications for monsoon
345 paleoclimatology. *Quaternary Research* 51, 215–219.
- 346 8. Chen, T., Xie, Q., Xu, H., Chen, J., Ji, J., Lu, J., Lu, H and Balsam, W, 2010, Characteristics
347 and formation mechanism of pedogenic hematite in Quaternary Chinese loess and
348 paleosols, *Catena* 81, 217-225.



- 349 9. Chlachula, J., Little, E., 2011, A high-resolution Late Quaternary climatostratigraphic
350 record from Iskitim, Priobie Loess Plateau, SW Siberia, *Quaternary International* 240 ,
351 139e149
- 352 10. Ding, Z.L., Ranov, V., Yang, S.L., Finaev, A., Han, J.M., Wang, G.A., 2002. The loess
353 record in southern Tajikistan and correlation with Chinese loess. *Earth and Planetary
354 Science Letters* 200, 387e400.
- 355 11. Ding, Z.L., Yang, S.L., Sun, J.M., Liu, T.S., 2001. Iron geochemistry of loess and Red
356 Clay deposits in the Chinese Loess Plateau and implications for long-term Asian monsoon
357 evolution in the last 7.0 Ma. *Earth and Planetary Science Letters* 185, 99–109.
- 358 12. Fischer, P., Hilgers, A., Protze, J., Kels, H., Lehmkuhl, F., Gerlach, R., 2012. Formation
359 and geochronology of Last Interglacial to Lower Weichselian loess/palaeosol sequences
360 — case studies from the Lower Rhine Embayment, Germany. *E & G Quat.Sci. J.* 61, 48–
361 63.
- 362 13. Fitzsimmons, K.E., Marković, S.B., Hambach, U., 2012. Pleistocene environmental
363 dynamics recorded in the loess of the middle and lower Danube Basin. *Quat. Sci. Rev.*
364 41,104–118.
- 365 14. Forster, T., Evans, M.E., Havlíček, P., Heller, F., 1996. Loess in the Czech
366 Republic:magnetic properties and paleoclimate. *Stud. Geophys. Geod.* 40, 243–261.
- 367 15. Frechen, M., Kehl, M., Rolf, C., Sarvati, R., Skowronek A., 2009, Loess Chronology of
368 the Caspian Lowland in Northern Iran, *Quaternary International*, No. 198, pp. 220-233.
- 369 16. Frechen, M., Oches, E.A., Kohfeld, K.E., 2003. Loess in Europe—mass accumulation rates
370 during the Last Glacial Period. *Quaternary Science Reviews* 22, 1835–1875.
- 371 17. Gallet, S., Jahn, B.M., Torii, M., 1996. Geochemical characterization of the Luochuan
372 loess-paleosol sequence, China, and paleoclimatic implications. *Chemical Geology* 133,
373 67–88.
- 374 18. Gocke, M., Hambach, U., Eckmeier, E., Schwark, L., Zöller, L., Fuchs, M., Löscher, M.,
375 Wiesenberg, G.L.B., 2014. Introducing an improved multi-proxy approach for
376 paleoenvironmental reconstruction of loess–paleosol archives applied on the Late
377 Pleistocene Nussloch sequence (SW Germany). *Palaeogeogr. Palaeoclimatol. Palaeoecol.*
378 410, 300–315.
- 379 19. Guanhua, L, Dunsheng, X, Ming, J, Jia, J, Jiabo, L, Shuang Z, Yanglei, W, 2014, Magnetic
380 characteristics of loesspaleosol sequences in Tacheng, northwestern China, and their
381 paleoenvironmental implications, *Quaternary International*, 3, 1-10.
- 382 20. Guo, Z.T., Ruddiman, W.F., Hao, Q.Z., Wu, H.B., Qiao, Y.S., Zhu, R.X., Peng, S.Z., Wei,
383 J.J., Yuan, B.Y., and Liu, T.S., 2002. Onset of Asian desertification by 22 Myr ago inferred
384 from loess deposit in China. *Nature* Vol. 416, pp. 159–163.
- 385 21. Heller, F., Liu, T., 1984. Magnetism of Chinese loess deposits. *Geophys. J. R. Astron. Soc.*
386 77, 125–141.
- 387 22. Hošek, J, Hambach, U, Lisá, L, Matys G. T, Horáček, I, 2015, an integrated rock-magnetic
388 and geochemical approach to loess/paleosol sequences fromBohemia andMoravia (Czech
389 Republic): Implications for the Upper Pleistocene paleoenvironment in central Europe,
390 *Palaeogeography, Palaeoclimatology, Palaeoecology* 418, 344–358.
- 391 23. Jary, Z., Ciszek, D., 2013. Late Pleistocene loess–palaeosol sequences in Poland and
392 western Ukraine. *Quat. Int.* 296, 37–50.
- 393 24. Jordanova, D., Grygar, T., Jordanova, N., Petrov, P., 2011. Palaeoclimatic significance of
394 hematite/goethite ratio in Bulgarian loess–palaeosol sediments deduced by DRS and rock



- 395 magnetic measurements. In: Petrovsky, E., Ivers, D., Harinarayana, T., Herrero- Bervera,
396 E. (Eds.), the Earth's Magnetic Interior. IAGA Special Sopron Book Series. Springer-
397 Verlag, Berlin.
- 398 25. Karimi, A., Khademi, H., Ayoubi, A., 2013, Magnetic susceptibility and morphological
399 characteristics of a loess–paleosol sequence in northeastern Iran, *Catena*, 101, pp. 56-60.
- 400 26. Karimi, A., Khademi, H., Jalalian, A., 2011, Loess: Characterize and application for
401 paleoclimate study, *Geography Research*, Volume 76, pp1-20.
- 402 27. Karimi, A., Khademi, H., Kehl, M., Jalaian, A., 2009, Distribution, Lithology and
403 Provenance of Peridesert Loess Deposits in Northeast Iran, *Geoderma*, No.148, pp. 241-
404 250.
- 405 28. Kehl, M., Frechen, M., Skowronek, A., 2005, Paleosols Derived from Loess and Loess-
406 like Sediments in the Basin of Persepolis, Southern Iran, *Quaternary International*,
407 No.140/141, pp.135-149.
- 408 29. Kehl, M., Sarvati, R., Ahmadi, H., Frechen, M., Skowronek, A., 2006, Loess /
409 Paleosol sequences along a Climatic Gradient in Northern Iran, *Eiszeitalter und Gegenwart*,
410 No. 55, pp.149-173.
- 411 30. Lateef, A.S.A., 1988. Distribution, provenance, age and paleoclimatic record of the loess
412 in Central North Iran. In: Eden, D.N., Furkert, R.J. (Eds.), *Loess – its Distribution, Geology
413 and Soil. Proceeding of an International Symposium on Loess, New Zealand, 14–21
414 February 1987*. Balkema, Rotterdam, pp. 93–101.
- 415 31. Mehdipour, F., 2012, Investigation of paleoclimate in late quaternary western alborz using
416 of technical applied and magnetism parameters, *Geology and Mineral Exploration*, master
417 science thesis.
- 418 32. Nabavi, Mehdi, 1976, *Introduction geology of Iran*, pp1-109.
- 419 33. Okhravi, R. Amini, A., 2001, Characteristics and Provenance of the Loess Deposits of the
420 Gharatikan Watershed in Northeast Iran, *Global and Planetary Change*, No. 28, pp.11-22.
- 421 34. Pashaei, A., 1996, Study of Chemical and Physical and Origin of Loess Deposits in Gorgan
422 and Dasht Area, *Earth Science*, 23/24, pp. 67-78.
- 423 35. Prins, M.A., Vriend, M., Nugteren, G., Vandenberghe, J., Huazu, L., Zheng, H., Weltje,
424 G.J., 2007. Late Quaternary aeolian dust input variability on the Chinese Loess Plateau:
425 inference from unmixing of loess grain-size record. *Quaternary Science Reviews* 26, 230–
426 242.
- 427 36. Schatz, A.-K., Scholten, T., Kühn, P., 2014. Paleoclimate and weathering of the Tokaj (NE
428 Hungary) loess–paleosol sequence: a comparison of geochemical weathering indices and
429 paleoclimate parameters. *Clim. Past Discuss.* 10, 469–507.
- 430 37. Song, Y., Shi, Z., Dong, H., Nie, J., Qian, L., Chang, H. & Qiang, X., 2008- Loess Magnetic
431 Susceptibility in Central Asia and its Paleoclimatic Significance. *IEEE International
432 Geoscience & Remote Sensing Symposium, II 1227-1230*, Massachusetts.
- 433 38. Spassov, S., 2002. Loess Magnetism, Environment and Climate Change on the Chinese
434 Loess Plateau. *Doctoral Thesis, ETH Zürich*, pp. 1–151.
- 435 39. Taylor, S.R., McLennan, S.M., McCulloch, M.T., 1983. Geochemistry of loess, continental
436 crustal composition and crustal model ages. *Geochimica et Cosmochimica Acta* 47, 1897–
437 1905.